



## Support parameters design of Jeffcoat rotor using nonlinear energy sink & $H^\infty$ method

H. Heidari<sup>1\*</sup>, P. Safarpour<sup>2</sup>

<sup>1</sup> Faculty of Mechanical Engineering, Malayer University, Malayer, Iran.

<sup>2</sup> Faculty of Mechanical & Energy Engineering, Shahid Beheshti University, Tehran, Iran.

**ABSTRACT:** Rotating machinery support design with the aim of robustly absorbing transient disturbances over a broad range of frequencies has significant importance regarding the various applications of this machinery. Hence, the nonlinear energy sink may be regarded as an efficient passive absorber, possessing adaptivity to the frequency content of vibrations of the primary system. This paper studies the effect of nonlinear energy sinks on the vibration suppression of a flexible rotor supported by a linear damping and an essentially nonlinear stiffness. First, the governing equations for the Jeffcott rotor model mounted on flexible supports are derived and numerically solved. Then, the optimal parameters for the linear supports have been analytically achieved by  $H^\infty$  optimization procedure. Numerical simulations have been performed to optimize the nonlinear energy sink parameters by using Matlab software in order to obtain the optimum performance for vibration reduction. Moreover, the  $H^\infty$  optimum parameters such as tuning frequency and damping ratios are expressed based on fixed-point theory to minimize the rotor amplitudes. It is proven by numerical simulations that the system optimization design can effectively improve the synchronous unbalance response.

### Review History:

Received: Feb. 10, 2020

Revised: May, 20, 2020

Accepted: Aug, 18, 2020

Available Online: Sep. 05, 2020

### Keywords:

$H^\infty$  optimization

Nonlinear energy sink

Jeffcott rotor

Support designs

Optimal absorber

### 1- Introduction

Reduction of whirling vibration amplitude generated by residual unbalance forces is necessary to keep the rotating machinery safe and efficient performance. The problem becomes more severe as machinery is designed to be lighter and faster. In order to increase performance requirements in various fields such as gas turbines, process equipment, auxiliary power machinery, and space applications, the engineer is faced with the problem of designing a unit capable of smooth operation under various conditions of speed and load. The rotor supports have a large influence on the behavior of rotating machinery and are able to efficiently reduce the resonant amplitude of the rotor systems when the stiffness and damping ratios are optimized appropriately.

The most popular solution in a vibration absorption and mitigation design is the linear Tuned Mass Damper (TMD). This solution is based on the linear dynamic system composed of a mass, a spring, and a damper attached to the linear or weakly nonlinear structure for the purpose of mitigating its vibration in the neighborhood of a single frequency [1]. The linear absorber has been widely utilized in different fields [2-4] since the process is developed by Frahm and Den Hartog [5]. It is a simple and efficient device but is questionable when several vibration modes of the primary structure have to be attenuated. This feature makes the design of vibration

absorbers a particularly challenging problem. In this context, Borges [2], Lu [3], and Habib [4] represented an interesting frequency-robust absorber by employing a non-linear system for the TMD.

More recent developments in passive technique for reducing vibration are to use purely non-linear absorbers relying on the principle of Targeted Energy Transfer (TET) or Nonlinear Energy Sink (NES). The concept of nonlinear energy sink was first proposed by Vakakis and Gendelman [6, 7], in 2001. The NESs have a linear damping and an essentially nonlinear stiffness. Several theoretical and experimental studies [8-10] have shown that passive targeted energy transfer, also referred to as the energy pumping phenomenon, can reduce or even passively eliminate vibration in the primary system. Theoretical and numerical studies have demonstrated that the use of strongly nonlinear attachments may produce dynamical regimes which are unavailable in common linear systems or systems with weak nonlinearity. It has been shown that properly designed nonlinear attachments may passively absorb and dissipates energy generated by transient disturbances, acting as nonlinear energy sinks. In references [11-13], the theoretical analysis of the effective energy absorption by NESs is realized over a relatively broad frequency range, making it effective over a range of frequencies. Previous literature has also shown that, unlike common linear and weakly nonlinear systems, the NESs can react efficiently on the amplitude characteristics of the

\*Corresponding author's email: hr.heidari@malayeru.ac.ir



external forcing in a wide range of frequencies. Hence, the NES may be regarded as efficient passive support, possessing versatility to reduce effectively vibration of the rotor-bearing system in an operating speed range.

Ahmadabadi and Khadem [14] studied the performance of the nonlinear energy sink for vibration mitigation of a drill string. The efficiency of various models of the drill-string and NESs were investigated, hence, the optimal parameters of the system for the maximum dissipated energy in the NES were extracted. They indicated that the dynamic stability of the drill-string is improved using the NESs. Georgiades et al. [15] presented systematically, passive broadband targeted energy transfers from a linear elastic continuum to an attached ungrounded NES. Bab et al. [16] studied the efficiency of a number of nonlinear energy sinks as nonlinear absorbers on the vibration reduction of a rotor-bearing system under mass eccentricity force. The NESs have a linear damping and essentially nonlinear stiffness. The equations of motion are derived for modeling of Jeffcott rotor by using Newton's second law. Guo et al. [17] investigated numerically, the efficiency of a passive targeted energy transfers to mitigate the whirling vibration amplitude in rotor systems at critical speeds.

In order to achieve this interesting phenomenon, the nonlinear stiffness and linear damping components of the NES should be optimized. One common optimization method is the  $H_\infty$  optimization that aims at minimizing the resonant vibration amplitude of the dynamic structure. The standard  $H_\infty$  optimum design method is based on fixed-point theory which is well documented for Dynamic Vibration Absorber (DVA) optimization of SDOF system by Den Hartog [5]. The objective is to minimize the maximum amplitude response of the primary system.

Heidari and Safarpour [18-19] established an analytical solution to the  $H_\infty$  and  $H_2$  optimization problems of DVA applied to suppress vibrations in Jeffcott rotor. The optimum flexibility and damping coefficients of the flexible rotor on linear support are obtained in order to minimize vibrational amplitudes and force transmissibility in the vicinity of the rotor's first critical speed.

Extending the concept of the vibration absorber as support to the nonlinear case, a very powerful method of reducing unwanted vibration is achieved by attaching a nonlinear energy sink to the system. According to the role of non-linear absorbers for suppressing vibration of structures, the purpose of the current research is to evaluate the influence of flexible supports on rotor amplitude. Although NESs have been successfully applied in many fields as discussed above works, to our knowledge, they have not been applied to vibration attenuation of rotor systems as flexible support, which motivates us to survey the application of the NES in rotor-bearing system field. Hence, the application of an optimal nonlinear energy sink as flexible support has significant importance in vibration mitigation of rotor-bearing systems.

In this investigation, the governing equations of motions for both NES-rotor and linear support-rotor dynamical systems have been derived using Newton's equations. Then,

the optimal parameters for the linear supports have been analytically obtained by  $H_\infty$  optimization method. The  $H_\infty$  optimum parameters such as tuning frequency and damping ratios are expressed based on fixed-point theory to minimize the vibration amplitude of the rotor. Furthermore, based on these analytical results, numerical simulations have been performed to optimize the NES parameters in order to attain the enhanced performance for vibration reduction. Numerical simulations demonstrate that the NES is able to efficiently reduce the whirling vibration amplitudes of rotor systems when the stiffness and damping ratios are optimized properly. For comparison purposes, vibration suppression during the passage through the critical speed has been investigated, first using the NES with purely cubic nonlinearity and then by using the linear stiffness. In addition, significant conclusions have been observed by using NES as flexible support in the rotor-bearing systems.

## 2- Flexible Rotor Dynamics Equation

A typical rotating system is composed of various components, such as rotors, disks, bearings, and supports. The dynamic response of a rotor-bearing system can be obtained by the set of differential equations from the Euler-Lagrange equations. The system parameters including the inertia properties of the rigid disk, stiffness of the rotating shaft, coefficients of bearing, and supports all of which have a significant influence on the dynamic characteristics of the rotor-bearing system.

In this investigation, a typical Jeffcott rotor is considered to be mounted on two journal bearings and two NESs as flexible, damped supports, which is composed of a small mass attached via strongly nonlinear spring and linear viscous damper. It can be assumed that the shaft is massless and the mass of the rotor is concentrated in a disk mounted at the rotor center. The schematic diagram and coordinates of the cross-section at the mid-span of the shaft are shown in Fig. 1. The support motion of either end of the rotor is given by the absolute coordinates  $(X_a, Y_a)$  and the bearing motion is denoted by  $(X_j, Y_j)$  in the fixed coordinate system. The rotor motion at the mid-span is described in the coordinate system by  $(X_d, Y_d)$ . The support and bearing characteristics are assumed to be symmetric to simplify the analysis of this rotor-bearing system.

Neglecting rotor acceleration and the disk gyroscopic, the governing equations of motion for the rotor, bearings, and support system in complex notation reduce to the following equation:

$$\begin{cases} m_a \ddot{z}_a + c_a \dot{z}_a + k_a z_a + k_{nl} z_a^3 + k_b (z_a - z_j) = 0 \\ m_d \ddot{z}_d + k_s (z_d - z_j) = m_d e \omega^2 e^{i\omega t} \\ k_b (z_j - z_a) + k_s (z_j - z_d) = 0 \end{cases} \quad (1)$$

$$\xrightarrow{\text{Matrix Form}} M\ddot{Z} + C\dot{Z} + KZ + f(Z) = F(t)$$

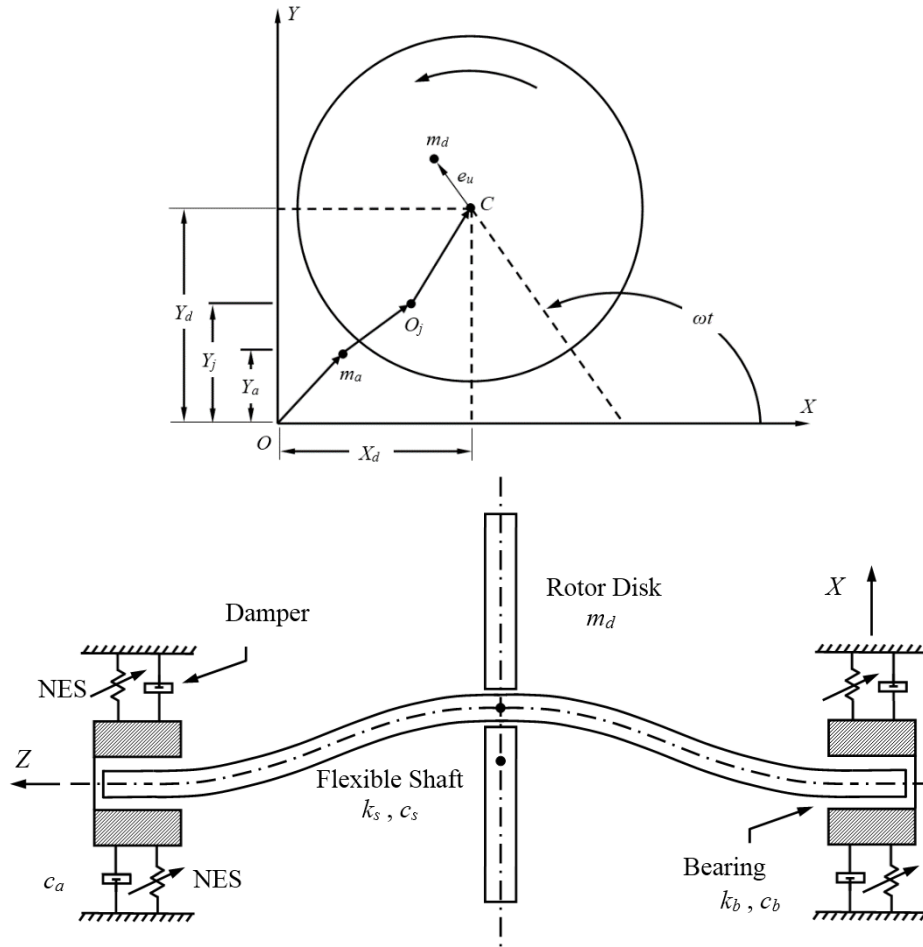


Fig. 1. Schematic diagram of Jeffcott rotor, journal bearings, and nonlinear energy sinks as flexible supports

where  $M$ ,  $C$  and  $K$  are the system mass, damping coefficient, and stiffness matrices respectively, can be represented by:

$$\begin{aligned}
 M &= \begin{bmatrix} m_a & 0 & 0 \\ 0 & m_d & 0 \\ 0 & 0 & 0 \end{bmatrix}, \\
 C &= \begin{bmatrix} c_a + c_b & 0 & -c_b \\ 0 & c_s & -c_s \\ -c_b & -c_s & c_s + c_b \end{bmatrix}, \\
 K &= \begin{bmatrix} k_b & 0 & -k_b \\ 0 & k_s & -k_s \\ -k_b & -k_s & k_s + k_b \end{bmatrix}
 \end{aligned} \quad (2)$$

Also, the non-linear spring forces acting on the supports,  $f(Z)$  have a hardening characteristic and are expressed as:

$$f(Z) = \begin{Bmatrix} f(z_a) \\ 0 \\ 0 \end{Bmatrix}, \quad f(z_a) = k_a z_a + k_{nl} z_a^3 \quad (3)$$

In Eqs. (1) and (2),  $m_d$  and  $m_a$  are the disk and support masses respectively. Damping and stiffness coefficients for the rotor shaft, bearings, and supports are denoted by  $c_s, k_s$  and  $c_b, k_b$  and  $c_a, k_a, k_{nl}$ , respectively. The rotor displacement vector,  $Z$  and Force vector,  $F$ , according to the rotor model become

$$F = \begin{Bmatrix} 0 \\ m_d e \omega^2 \\ 0 \end{Bmatrix} e^{i\omega t}, \quad Z = \begin{Bmatrix} z_a \\ z_d \\ z_j \end{Bmatrix} \quad (4)$$

A general trend for the development of numerical

analytical methods is to avoid unnecessary complications. Hence, linear methods of analysis are preferable. The straight linearization method presented in this article is a numerical-analytical method for the prediction of the steady-state periodic response. Using this method, the set of nonlinear differential equations governing the motion of rotor systems is transformed into a set of nonlinear algebraic equations. After the initial transient motion has damped out, the steady-state unbalance response may be assumed  $Z_k = A_k e^{i\omega t}$  in which  $A_k$  is in general complex. By applying the method of straight linearization [20], the nonlinear spring characteristics are represented as linear functions  $k_a^* X$ , which are obtained by minimizing the functional

$$I(k_a^*) = \int [f(X) - k_a^* X]^2 X^2 dX \quad (5)$$

and the expressions for  $k_a^*$  are

$$k_a^* = (5/A_a^5) \int f(X) X^3 dX \quad (6)$$

By substituting Eq. (6) into Eq. (1) and rearranging, the differential equations of motion may be reduced to a set of algebraic equations for the determination of the rotor steady-state motion. It is assumed that the damping coefficients  $c_s$  and  $c_b$  are equal to zero for simplicity, therefore one can write:

$$\begin{aligned} (-m_a \omega^2 + i c_a \omega + k_a + k_b) A_a + 5k_{nl} A_a^3 / 7 - k_b A_j &= 0 \\ (-m_d \omega^2 + k_s) A_d - k_s A_j &= m_d e \omega^2 \\ -k_b A_a - k_s A_d + (k_b + k_s) A_j &= 0 \end{aligned} \quad (7)$$

For simplicity and better interpretation (more convenient explanation) of governing equations, the following dimensionless parameters are defined:

$$\begin{aligned} \beta &= k_b / k_a, \quad \mu = k_s / k_b, \quad \gamma = k_{nl} / k_a \\ \omega_n^2 &= k_s / m_d, \quad \omega_a^2 = k_a / m_a \\ \Omega_a &= \omega / \omega_a, \quad \Omega = \omega / \omega_n \\ c_{ca} &= 2\sqrt{k_a m_a}, \quad \zeta = c_a / c_{ca} \end{aligned} \quad (8)$$

where  $\omega$  is the rotating speed and a new ratio  $\alpha = \frac{\omega_a}{\omega} = \frac{\Omega}{\Omega_a}$  is defined. Then Eq. (7) become Eq. (9) can be written in terms of non-dimensional quantities as follow:

$$\begin{aligned} (\alpha^2 + \beta \alpha^2 - \Omega^2 + i 2\zeta \Omega) A_a + \\ 5\gamma \alpha^2 A_a^3 / 7 - \beta \alpha^2 A_j &= 0 \\ (1 - \Omega^2) A_d - A_j &= e \Omega^2 \\ -A_a - \mu A_d + (1 + \mu) A_j &= 0 \end{aligned} \quad (9)$$

In the algebraic Eq. (9), there is only one non-linear term which is  $A_a^3$ . Therefore, taking the amplitude  $A_a$  and the angular frequency  $\Omega$  as the master parameters, closed-form expressions can be easily obtained for the response surfaces.

In the linear case, the rotor amplitude can be obtained as the following equation:

$$\frac{A_d}{e \Omega^2} = \frac{(1 - \Omega_a^2)(1 + \mu) + \mu \beta + (2i \zeta \Omega_a)(1 + \mu)}{H_1(1 - \Omega_a^2) - \mu \beta \Omega^2 + (2i \zeta \Omega_a) H_1} \quad (10)$$

Since the support amplitude in the frequency domain is given by:

$$\frac{A_a}{e \Omega^2} = \frac{\mu \beta}{H_1(1 - \Omega_a^2) - \mu \beta \Omega^2 + (2i \zeta \Omega_a) H_1} \quad (11)$$

where

$$H_1 = [1 - \Omega^2(1 + \mu)] \quad (12)$$

### 3- Optimal Design Procedure

The successful design of the rotor-bearing system needs to be analyzed with respect to the optimal parameters of the dynamic support. It is, therefore, highly desirable to have an easily applied method to obtain an estimate of the optimum bearing damping for synchronous response. Multiple constraints such as the placement of critical speeds, minimization of response amplitudes and bearing loads, optimal choice of balance planes, and maximization of the onset of instability speed, are used to meet the engineering requirements

In this work, synchronous unbalance response in the operational speed range is the objective function. Many numerical optimization methods have been developed and used for the design optimization of rotor-bearing systems. Most of these optimization methods are cumbersome.

One common optimization method is the  $H_\infty$  optimization that aims at minimizing the resonant vibration amplitude of the dynamic structure. The standard  $H_\infty$  optimum design method is based on fixed-point theory which is well documented for dynamic vibration absorber optimization of SDOF system by Den Hartog [5]. The objective is to minimize the maximum amplitude response of the primary system. Therefore, the approach method is a highly desirable and easily applied method to obtain an estimate of the optimum bearing stiffness and damping.

#### 3-1- H-infinity optimization for minimizing Synchronous Response

In the linear case, to determine how effective the flexible support is in attenuating the rotor amplitude, a new ratio  $\alpha = \frac{\omega_a}{\omega_n} = \frac{\Omega}{\Omega_a}$  is defined. Then Eq. (10) becomes:

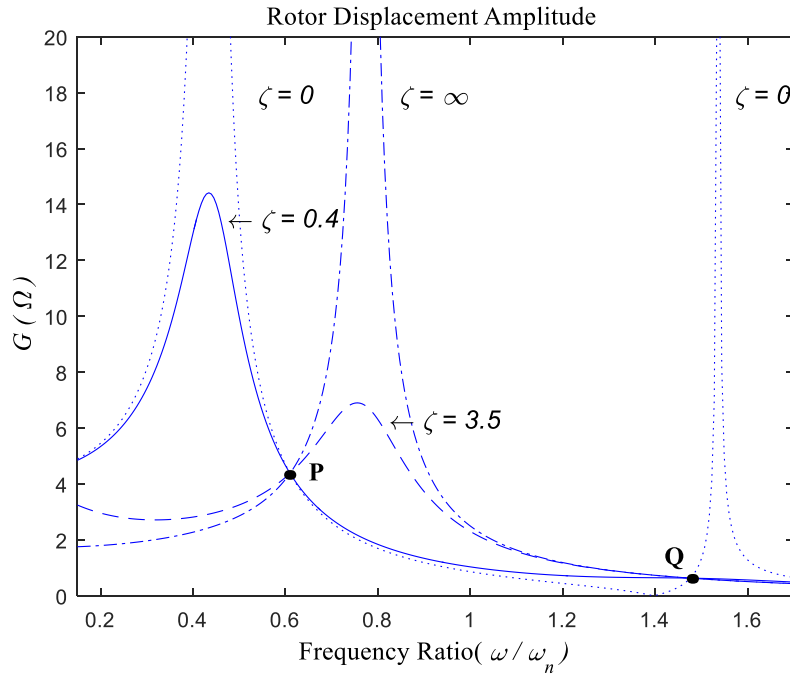


**Fig. 2. Absolute rotor motion with  $\mu = 0.67$  ,  $\alpha = 0.86$  and  $\beta = 4$  for various values of support damping**

$$G(\Omega) = \frac{A_d}{e\Omega^2} = \left\{ \frac{[(\alpha^2 - \Omega^2)(1 + \mu) + \mu\alpha^2\beta]^2 + [2\zeta\alpha\Omega(1 + \mu)]^2}{[H_1(\alpha^2 - \Omega^2) - \mu\beta\alpha^2\Omega^2]^2 + [2\zeta\alpha\Omega H_1]^2} \right\}^{1/2} \quad (13)$$

In considering  $H_\infty$  optimization for a specific point, the objective is to minimize the maximum forces transmitted by the primary system to the excitation force.

$$\max(|G(\Omega, \alpha_{H_\infty}, \zeta_{H_\infty})|) = \min(\max|G(\Omega)|) \quad (14)$$

$G(\Omega)$  is calculated according to Eq. (13) with four damping ratios, and the results are shown in Fig.2. Note that all curves pass through two points P, Q on the graph, independent of the damping parameter  $\zeta$ , and these points are known as fixed points.  $H_\infty$  optimization can be derived based on the fixed-point theory that expresses in the frequency response spectrum. Therefore, the  $H_\infty$  optimum condition may be expressed as:

$$\begin{aligned} \max(|G(\Omega, \alpha_{H_\infty}, \zeta_{H_\infty})|) = \\ \min(\max(|G(\Omega_P)|, |G(\Omega_Q)|)) \end{aligned} \quad (15)$$

In the other words, support parameters  $\alpha_{H_\infty}$  and  $\zeta_{H_\infty}$  are achieved when the fixed points are adjusted to equal height and become the peaks of the motion amplitude.

The dimensionless frequencies of the points P and Q are independent of the value of  $\zeta$  if the ratio of the coefficient of  $\zeta^2$  to the term independent of  $\zeta$  is the same in both numerator and denominator of Eq. (13).

$$\frac{[2\alpha\Omega(1 + \mu)]^2}{[(\alpha^2 - \Omega^2)(1 + \mu) + \mu\alpha^2\beta]^2} = \frac{[2\alpha\Omega H_1]^2}{[H_1(\alpha^2 - \Omega^2) - \mu\beta\alpha^2\Omega^2]^2} \quad (16)$$

The Eq. (16) is satisfied if:

$$\begin{aligned} (2\alpha\Omega)^2 = 0, \\ \frac{(1 + \mu)}{(\alpha^2 - \Omega^2)(1 + \mu) + \mu\alpha^2\beta} - \frac{H_1}{H_1(\alpha^2 - \Omega^2) - \mu\beta\alpha^2\Omega^2} = 0, \\ \frac{(1 + \mu)}{(\alpha^2 - \Omega^2)(1 + \mu) + \mu\alpha^2\beta} + \frac{H_1}{H_1(\alpha^2 - \Omega^2) - \mu\beta\alpha^2\Omega^2} = 0 \end{aligned} \quad (17)$$

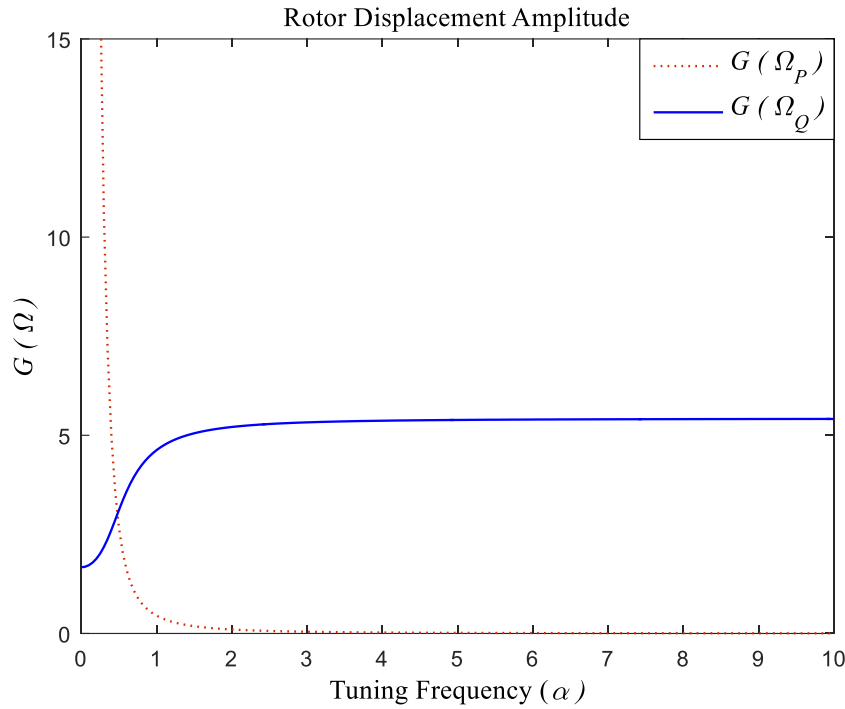


**Fig. 3. The height of the fixed points versus tuning frequency  $\alpha$  at  $\mu = 0.67$  and  $\beta = 4$**

The first two solutions are trivial. The third yields the Eq. (18).

$$(1+\mu)^2 \Omega^4 - b(1+\mu)\Omega^2 + (1+\mu + \mu\beta/2)\alpha^2 = 0, \tag{18}$$

$$b = [\alpha^2(1+\mu + \mu\beta) + 1]$$

The solution of this equation gives two values of  $\Omega$ , designated  $\Omega_c$ , one corresponding to each fixed point. The dimensionless frequencies of the points P and Q are obtained as follow:

$$\Omega_{p,q}^2 = \frac{b \pm \sqrt{b^2 - 4\alpha^2(1+\mu + \mu\beta/2)}}{2(1+\mu)} \tag{19}$$

$$\Rightarrow \Omega_p^2 + \Omega_Q^2 = \frac{b}{(1+\mu)}$$

The unbalance response  $G(\Omega)$  at each fixed point may be found by substituting each value of  $\Omega_c$  given by Eq. (19) into Eq. (13). Since the amplitude is independent of  $\zeta$ , the value that gives the simplest calculation (namely,  $\zeta = \infty$ ) can be used for the calculation as below:

$$G(\Omega)|_{p,q} = \left\{ \frac{(1+\mu)^2}{[1 - \Omega_{p,q}^2(1+\mu)]^2} \right\}^{1/2} \tag{20}$$

In order to find the tuning frequency, the heights of the fixed points are calculated at different values of  $\alpha$  and the results are plotted in Fig. 3.

By comparing the height of the fixed points at different values of  $\alpha$  Fig. 4 may be found point A is the minimum of the graph and that is the case in which two fixed points have the same amplitude. In order to reach the optimum tuning, the responses at P and Q should be the same, therefore

$$|G(\Omega_p)| = |G(\Omega_Q)|$$

$$\Rightarrow \frac{(1+\mu)}{1 - \Omega_p^2(1+\mu)} = \frac{-(1+\mu)}{1 - \Omega_Q^2(1+\mu)} \tag{21}$$

That is

$$\Omega_p^2 + \Omega_Q^2 = \frac{2}{(1+\mu)} \tag{22}$$

The optimum value of  $\alpha$  is that for which the rotor



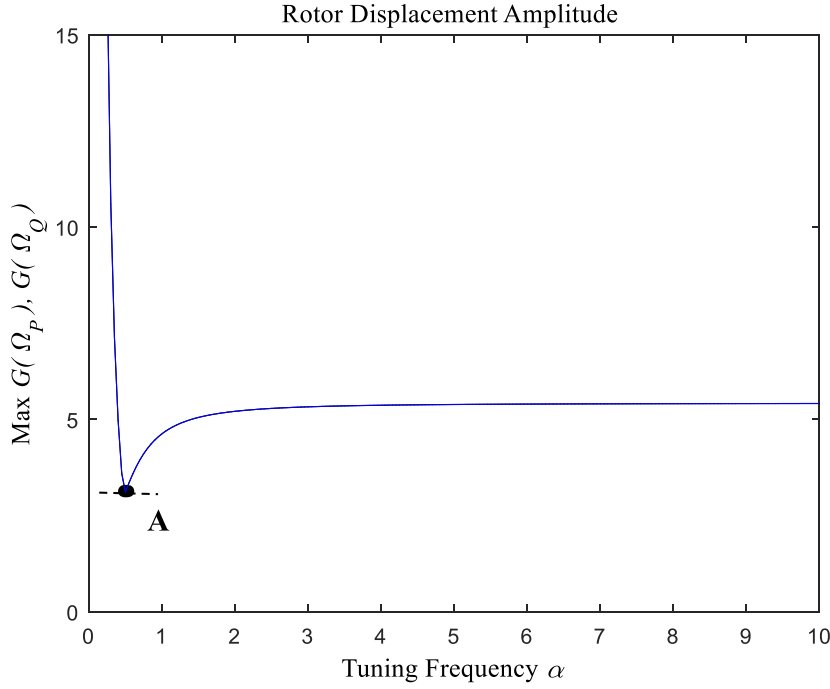


**Fig. 4. Maximum height of the fixed points versus tuning frequency  $\alpha$  at  $\mu = 0.67$  and  $\beta = 4$**

amplitude  $\left| \frac{A_i}{\Omega^2} \right|$  at P is equal to that at Q. From Eqs. (19) and (22) the optimum tuning condition is obtained as:

$$\alpha_{H_\infty \text{ optimization}} = \sqrt{\frac{1}{1 + \mu(1 + \beta)}} \quad (23)$$

If the effect of the damping is considered, it is possible to choose a value of the damping parameter  $\zeta$  that will make points P and Q the maximum points on the unbalance response. The condition of points P and Q being the maximum means that the rotor amplitude curve should pass through the two fixed points with a horizontal tangent, that is

$$\frac{\partial}{\partial \Omega^2} [G(\Omega)]^2 = 0 \quad (24)$$

Solving this equation for  $\zeta^2$  one obtains

$$\zeta^2 = \frac{H_1^2 H_2 - (1 + \mu)[H_1(\alpha^2 - \Omega^2) - \mu\beta\alpha^2\Omega^2][H_1 + H_2]}{H_1(1 + \mu)^2 [2\alpha\Omega]^2} \quad (25)$$

That is

$$H_2 = (1 + \mu)(\alpha^2 - \Omega^2) + \mu\beta\alpha^2 \quad (26)$$

A proper value for the maximum damping is obtained by solving for the value of  $\zeta$  in Eq. (25) when  $\Omega_{P,Q}^2$  is given by Eq. (19) and  $\alpha$  has the optimum value given by Eq. (23). This gives the following approximate value for the optimum damping parameter

$$\zeta_{P,Q}^2 = \frac{3}{4} \frac{\mu\beta(1 + \mu + \mu\beta)}{(1 + \mu)[2(1 + \mu + \mu\beta) \pm \sqrt{2\mu\beta(1 + \mu + \mu\beta)}]} \quad (27)$$

Taking an average of  $\zeta_P^2$  and  $\zeta_Q^2$  produces:

$$\zeta_{H_\infty \text{ optimization}}^2 = \frac{\zeta_P^2 + \zeta_Q^2}{2} = \frac{3}{4} \frac{\mu\beta(1 + \mu + \mu\beta)}{(1 + \mu)[2(1 + \mu + \mu\beta) - \mu\beta]} \quad (28)$$

In the more general, the single mass rotor theory can be applied to investigate optimum support flexibility  $\alpha_{opt}$  and damping  $\zeta_{opt}$  for multi-mass rotors operating below their second bending critical speed.

In the nonlinear case, the non-linear spring ratios  $\gamma$  are considered to be the design variables. The NES has a small mass and damping. Also, the damping of the NES is linear, but its stiffness is nonlinear. Furthermore, based on the analytical results of the linear case, numerical simulations

**Table 1. Parameters used for simulation [21]**

Parameter	Rotor	Roller Bearing	Support (Absorber)	Unit
Mass	44	-	22	(kg)
Damping Coefficient	0	0	30	(N.s/m)×10 <sup>3</sup>
Stiffness Coefficient	58	87.5	22	(N/m)×10 <sup>6</sup>
Unbalance load	0.045	-	-	(N)
Disk Radius	0.254	-	-	(m)

have been performed to optimize the NES parameter in order to obtain the optimum performance for vibration reduction. The approach method of the tuned damper support system is similar to that designed for dynamic vibration absorber optimization.

A nonlinear sink, on the other hand, can provide energy reduction over a much wider bandwidth and consequently can be more efficient in its implementation. Energy is important to consider in any system, how it is dissipated or added to a system over time can give some indication of the system dynamics and evolution. The mechanical energy of the system is composed of kinetic and potential energy. The kinetic energy arises from the motion of the system and the potential from the spring force acting on the mass. Further comparisons between the performances of each system can be made by observing the total system energy as a function of time. The total system energy is governed by:

$$\begin{aligned}
 E_{Linear} &= \frac{1}{2} \omega^2 (m_d A_d^2 + m_a A_a^2) + \frac{1}{2} k_a A_a^2 \\
 &\quad + \frac{1}{2} k_b (A_a - A_j)^2 + \frac{1}{2} k_s (A_d - A_j)^2 \\
 E_{NES} &= \frac{1}{2} \omega^2 (m_d A_d^2 + m_a A_a^2) + \frac{1}{4} k_a A_a^4 \\
 &\quad + \frac{1}{2} k_b (A_a - A_j)^2 + \frac{1}{2} k_s (A_d - A_j)^2
 \end{aligned} \tag{29}$$

The optimal parameters of the system for the dissipated energy in the NES are considered.

#### 4- Simulation Studies

In this section, the sophisticated procedure presented in section 3 is used for the optimum design of support parameters. In order to analyze the behavior of the rotor, results are presented for linear and nonlinear cases under the

resonance conditions. Fig. 1 shows a schematic of the Jeffcott model including the rotor, journal bearings, and nonlinear energy sinks as flexible supports. The parameters used in the simulation are given in Table 1.

The problem to be considered now will be the selection of an optimum value of stiffness and damping to use in the support to minimize rotor amplitude. First, the optimal parameters for the linear supports have been investigated based on  $H_\infty$  optimization procedure.

Fig. 5 represents the dynamic response versus the rotor speed for the optimum tuning  $\alpha$  in which the tuned support will cause the same magnitude of amplitude at both fixed points P and Q for several damping ratios. The support stiffness ratio is obtained  $\alpha_{H_\infty \text{ optimization}} = 0.4473$  from Eq. (23).

In addition to these steady-state conditions, the proper damper design must also take into consideration the optimum support damping. By selecting the optimum support stiffness and using Eq. (28), the magnitude of support damping coefficient will be  $\xi_{H_\infty \text{ optimization}} = 1.0607$  for  $H_\infty$  method. The magnitude of damping required has been determined, and it is now necessary to design the damper support to produce this amount of damping. Thereby optimum support damping will cause decreased vibrational amplitude. Fig. 6 shows the resultant minimum rotor amplitude with undamped support, infinite damping, and optimum damping ratio by  $H_\infty$  optimization procedure, respectively. It is obvious from the comparison that optimum damping will make points P and Q the maximum points on the  $|G(\Omega)|$ . Consequently, the maximum rotor amplitude of the system can be reduced by more than 50% for  $H_\infty$  optimization procedure while the optimum parameters are used.

Now optimization procedure is performed for the system with nonlinear stiffness and linear damping components in the flexible supports. From Eqs. (23) and (28), the magnitude of the tuning ratio  $\alpha_{opt}$  and the damping ratio  $\xi_{opt}$  are achieved, respectively. Only non-linear ratio  $\gamma$  is varied through the interval  $70 \leq \gamma \leq 85$  to attain the optimum performance for vibration reduction. The optimum non-linear ratio is obtained



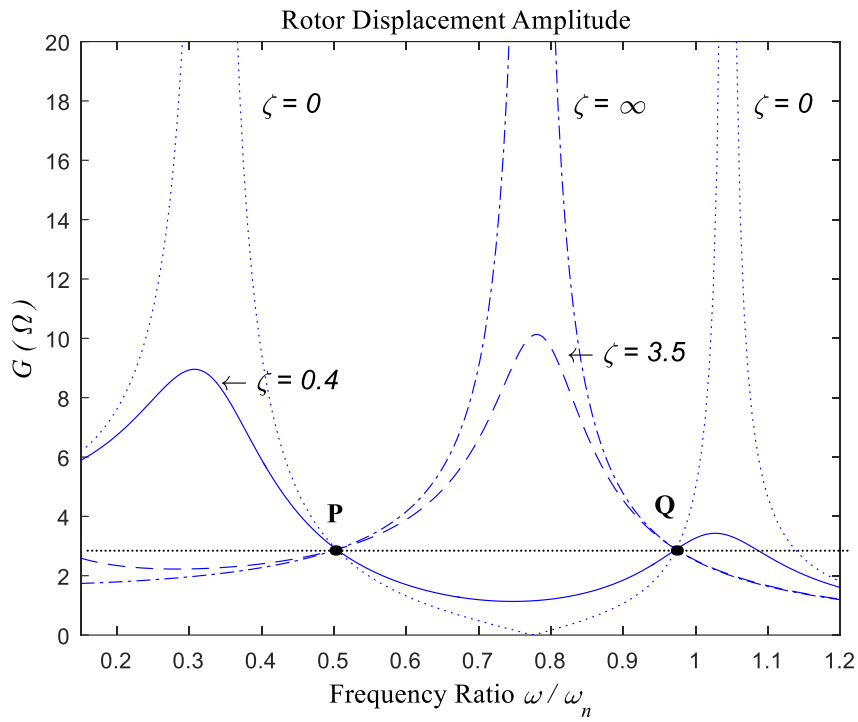


Fig. 5. Rotor amplitude with a tuned support system for various values of support damping

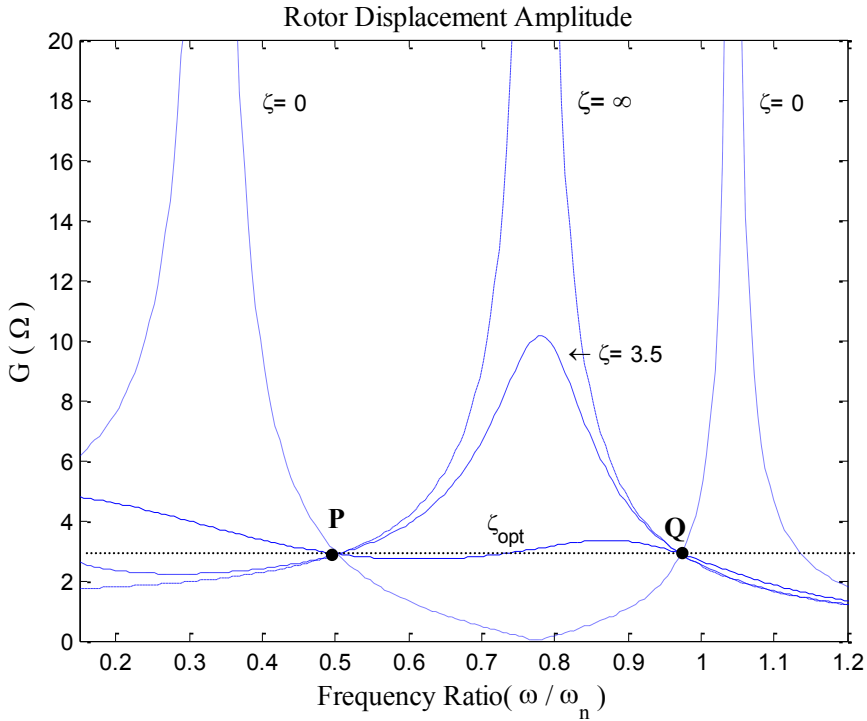
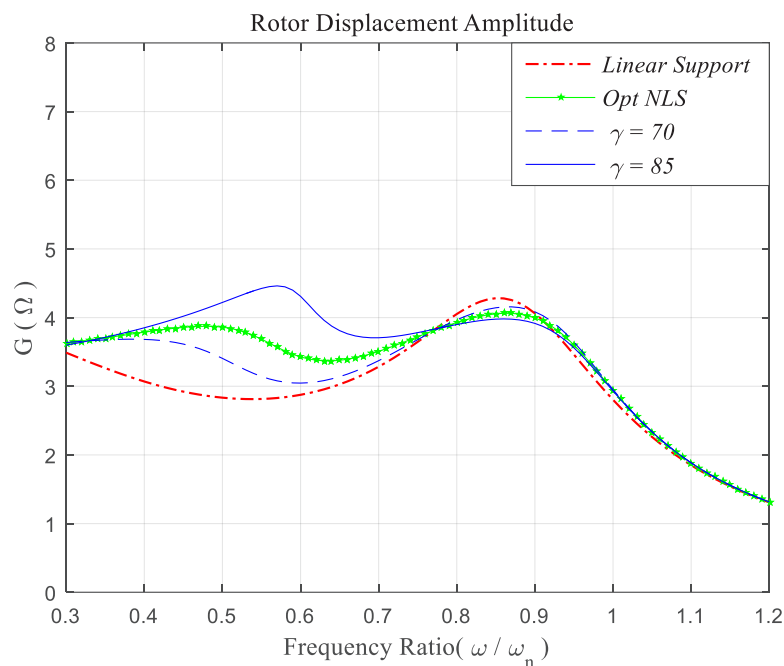


Fig. 6. Rotor amplitude with optimum support parameters by  $H_\infty$  optimization



**Fig. 7. Comparison of synchronous response for both linear and non-linear support with optimum parameters**

$\gamma = 75$  for  $\alpha_{opt} = 0.4473$  and  $\xi_{opt} = 1.0607$  with respect to whirling vibration amplitude as an objective function. A better comparison of different manner between linear and various Non-Linear Spring support (NLS) in minimizing the synchronous unbalance response, are shown in Fig. 7, one can see that some improvement is achieved in non-linear case. It can be seen that the modified NES support becomes a smoother transition from peak to peak than linear support.

The significant reduction in the vibration amplitudes of the primary system is clear at the beginning of oscillation in Fig. 8. This reduction is due to fact that the NES force is dominated by the negative stiffness components which makes this force act in the opposite direction of the motion of the primary mass, even though both of the systems and NES masses are moving in the same direction.

In order to demonstrate more clearly the effect of the NES, it would be interesting to consider the total system energy with linear and nonlinear supports. Fig. 9 illustrates that the NES performance as nonlinear support is remarkably enhanced in regards to vibration suppression compared with the linear support. As consequence, the energy in the system with the nonlinear spring support is lower than its linear spring one. The effects of the energy reduction are evident due to the decreased displacement of the main system. The presented results have shown that nonlinearly support with nonlinear spring is an attractive solution to mitigate the whirling vibration amplitude in rotor systems than the linear counterparts.

Consequently, even though the TMD performance is not affected by the level of total energy in the system, it is only effective when the frequency of a specified vibration mode to be attenuated is near to the natural frequency of the main system. In contrast to the linear and NES systems, the NES is applicable at energy dissipation with a much wider range of multiple resonant frequencies compared with the linear TMDs. Hence, the NES may be regarded as efficient passive support, possessing versatility to reduce effectively vibration of the rotor-bearing system in an operating speed range. This is due to the essential stiffness nonlinearity will be capable to engage intransient resonance with linear modes of the rotor system at arbitrary frequency ranges.

The effect of these parameters represents a tuned condition in which the designer enables to select the support appropriately. In general, theoretical data for a single-mass rotor can be used to determine flexible support properties to attenuate the vibration amplitude of the rotor and dynamic response for a multi-mass rotor operating through the first bending critical speed.

## 5- Conclusions

Extending the concept of the vibration absorber as support to the nonlinear case, a very powerful method of reducing unwanted vibration is achieved by attaching a nonlinear energy sink (NES) to the system. The application of an optimal nonlinear energy sink as flexible support in vibration mitigation of rotor-bearing systems was studied in this paper.

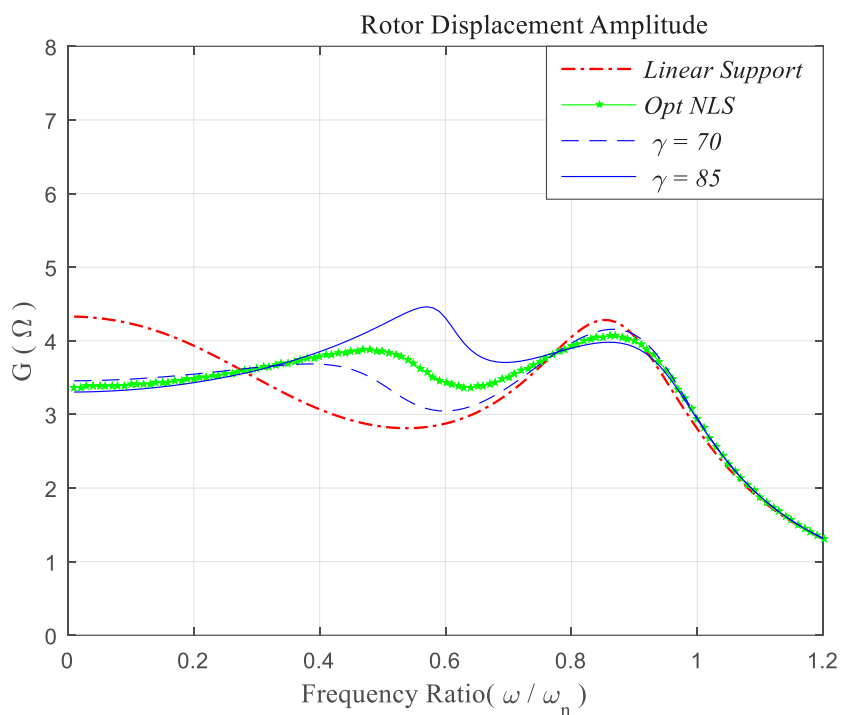


Fig. 8. Comparison between linear and various non-linear support at the beginning of the primary system oscillation

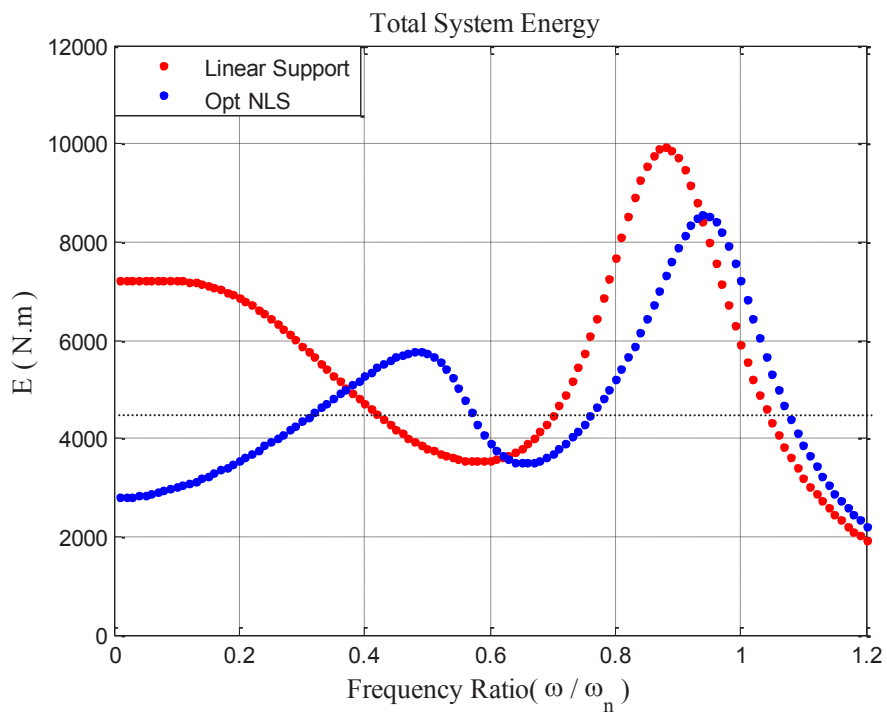


Fig. 9. Total system energy for both linear and non-linear support at  $\gamma = 75$

The governing equations for the Jeffcott rotor model mounted on flexible supports are derived and numerically solved by using Matlab software. The proposed method, based on  $H_{\infty}$  optimization procedure and numerical simulations has been performed to determine the optimum support flexibility and damping of a flexible rotor to minimize the rotor amplitude. It is proven by numerical simulations that the system optimization design can effectively improve the synchronous unbalance response. Moreover, it was shown that NES has significant performance on the vibration suppression of a flexible rotor-bearing supported by a linear damping and an essentially nonlinear stiffness. Finally, it was found that the total system energy with the nonlinear spring attachment is lower than its linear spring counterpart. The presented results have shown that the nonlinear system with nonlinear spring is an attractive occurrence to the design of supporting turbomachinery.

## References

- [1] L. Li, Y. Du, Design of nonlinear tuned mass damper by using the harmonic balance method, *Journal of Engineering Mechanics*, 146 (6) (2020) 04020056.
- [2] R.A. Borges, A.M. Lima, V. Steffen, Robust optimal design of a nonlinear dynamic vibration absorber combining sensitivity analysis, *Journal of Shock and Vibration*, 17 (2010) 507-520.
- [3] Z. Lu, Z. Wang, and Y. Zhou, Nonlinear dissipative devices in structural vibration control: a review, *Journal of Sound and Vibration*, 423 (2018) 18-49.
- [4] G. Habib, T. Detroux, R. Vigi e, G. Kerschen, Nonlinear generalization of Den Hartog's equal-peak method, *Mechanical Systems and Signal Processing*, 52 (2015) 17-28.
- [5] J.P. Den Hartog, *Mechanical Vibrations*, Fifth Ed., New York, Mc Graw-Hill, (1985).
- [6] O.V. Gendelman, L. I. Manevitch, A. F. Vakakis, and R. Mcloskey, Energy pumping in nonlinear mechanical oscillators: Part I - Dynamics of the underlying Hamiltonian systems, *Journal of Applied Mechanics*, 68 (2001) 34-41.
- [7] A. F. Vakakis, O.V. Gendelman, Energy pumping in nonlinear mechanical oscillators: Part II - Resonance capture, *Journal of Applied Mechanics*, 68 (2001) 42-48.
- [8] A. Amiri, M. Dardel, and H.M. Daniali, Effects of passive vibration absorbers on the mechanisms having clearance joints, *Multibody System Dynamics*, 47 (2019) 363-395.
- [9] M. Weiss, A. Savadkoochi, O. Gendelman, C. Lamarque, Dynamical behavior of a mechanical system including Saint-Venant component coupled to a non-linear energy sink, *International Journal of Non-Linear Mechanics*, 63 (2014) 10-18.
- [10] M. Farid, N. Levy, O.V. Gendelman, Vibration mitigation in partially liquid-filled vessel using passive energy absorbers, *ASME Journal of Sound and Vibration*, 406 (2017) 51-73.
- [11] G. Kerschen, J. J. Kowtko, D. M. McFarland, L. A. Bergman, A. F. Vakakis, Theoretical and experimental study of multimodal targeted energy transfer in a system of coupled oscillators, *Journal of Nonlinear Dynamics*, 47 (2007) 285-309.
- [12] Y. Liu, A. Mojahed, L.A. Bergman, A new way to introduce geometrically nonlinear stiffness and damping with an application to vibration suppression, *Nonlinear Dynamics*, 96 (2019) 1819-1845.
- [13] A. Blanchard, L. A. Bergman, and A. F. Vakakis, Targeted energy transfer in laminar vortex-induced vibration of a sprung cylinder with a nonlinear dissipative rotor, *Physica D: Nonlinear Phenomena*, 350 (2017) 26-44.
- [14] Z.N. Ahmadabadi, S.E. Khadem, Self-excited oscillations attenuation of drill-string system using nonlinear energy sink, *Journal of Mechanical Engineering Science*, 227 (2) (2012) 230-245.
- [15] F. Georgiades, A.F. Vakakis, G. Kerschen, Broadband passive targeted energy pumping from a linear dispersive rod to a lightweight essentially non-linear end attachment, *International Journal of Non-Linear Mechanics*, 42 (5) (2007) 773-788.
- [16] S. Bab, S. E. Khadem, M. Shahgholi, Vibration attenuation of a rotor supported by journal bearings with nonlinear suspensions under mass eccentricity force using nonlinear energy sink, *Meccanica*, 50 (9) (2015) 2441-2460.
- [17] C. Guo, M.A. AL-Shudeifat, A.F. Vakakis, Vibration reduction in unbalanced hollow rotor systems with nonlinear energy sinks, *Nonlinear Dynamic*, 79 (1) (2015) 527-538.
- [18] H.R. Heidari, P. Safarpour,  $H_{\infty}$  and  $H_2$  optimization procedures for optimal design of support parameters of a flexible rotor, *Computational and Applied Mathematics*, 38 (2019) 152.
- [19] H.R. Heidari, P. Safarpour, Optimal design of support parameters for minimum force transmissibility of a flexible rotor based on  $H_{\infty}$  and  $H_2$  optimization methods, *Engineering Optimization*, 50 (2018) 671-683.
- [20] I.S. Gradshteyn, I.M. Ryzhik, *Table of Integrals Series and Products*, Academic Press Inc., (1994).
- [21] Cunningham, R.E., E.J. Gunter. "Design of a squeeze film damper for a multi-mass flexible rotor." *Journal of Engineering for Industry*, 97 (4) (1975) 1383-1389.

### HOW TO CITE THIS ARTICLE

H. Heidari, P. Safarpour, A Support parameters design of Jeffcoat rotor using nonlinear energy sink &  $H_{\infty}$  method. *AUT J. Mech Eng.*, 5(2) (2021) 227-238.

DOI: 10.22060/ajme.2020.17847.5876

